

# Redox and Fluorophore Functionalization of Water-Soluble, Tiopronin-Protected Gold Clusters

Allen C. Templeton, David E. Cliffler, and Royce W. Murray\*

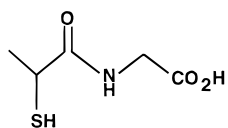
Contribution from the Kenan Laboratories of Chemistry, University of North Carolina, Chapel Hill, North Carolina 27599-3290

Received February 17, 1999

**Abstract:** Place-exchange and amide-forming coupling reactions represent two facile and efficient routes to poly-functionalization of water-soluble nanoparticles. In this paper, place-exchange and amide-forming coupling reactions with water-soluble tiopronin-MPCs are described and their products characterized by  $^1\text{H}$  and  $^{31}\text{P}$  NMR, capillary electrophoresis, electrochemistry, and fluorescence spectroscopy. Place-exchange reactions of ligands with tiopronin-MPCs yield products with about half of the ligand exchange expected on the basis of solution stoichiometry and a nonselective exchange and were not noticeably affected by steric encumbrances. Tiopronin-MPCs to which viologens are coupled (avg 36/MPC) adsorb as monolayers on Au electrodes as shown in electrochemical quartz crystal microbalance experiments. Multilayer adsorption occurs on long experimental time scales. The strong adsorption of the viologen-functionalized clusters is ascribed to increased interaction and stability in the viologen reduction products. Capillary electrophoresis experiments with tiopronin-MPCs and viologen-functionalized tiopronin-MPCs reveal a number of separable core size/charge state combinations. Fluorescence measurements show  $\sim 50\%$  quenching of fluorescein upon attachment (avg 3.7/cluster) to tiopronin-MPCs, relative to the monomer under the same conditions. The results of this paper provide a pathway to explore poly-functionalized water-soluble nanoparticles in a variety of applications, including their use as biosensors.

## Introduction

We recently described the synthesis and characterization of a water-soluble, monolayer-protected gold cluster (MPC) molecule,<sup>1</sup> in which the monolayer is composed of the simple compound "tiopronin" (*N*-2-mercaptopropionyl-glycine):



Tiopronin

The average composition of tiopronin-MPCs varies with reaction conditions. Those employed in this study have the average composition  $\text{Au}_{201}\text{Tiopronin}_{85}$ . While still exploiting the ease of the Brust reaction route to alkanethiolate MPCs,<sup>2</sup> synthesis of the tiopronin-protected Au clusters expands the chemistry of these materials into aqueous media.<sup>3</sup> The nanometer-sized tiopronin-MPCs offer possibilities as platforms for the design of aqueous analytical probes with significantly smaller dimensions than those of conventional gold colloids<sup>4,5</sup> and, at the same time, the potential advantages of versatile and flexible

functionalization. Alkanethiolate-MPCs have received considerable attention for their advantages of stability, isolability in dried forms that can be redissolved without aggregation, and facile characterization and functionalization.<sup>6,7</sup> Tiopronin-protected clusters have the same exceptional features, plus water solubility, but their further functionalization has not yet been accomplished. The present report addresses the latter need.

This paper describes a study of place-exchange and of amide-forming coupling reactions designed for the functionalization of tiopronin-MPCs. Chemical functionalization strategies for soluble and isolable nanoparticles have been the subject of only a few reports<sup>7d,e</sup> and are a largely unexplored topic. Place-exchange reactions of tiopronin-MPC ligands with other ligands in aqueous media were examined and compared to analogous reactions involving alkanethiolate MPCs.<sup>7a-c</sup> Amide-forming coupling reactions between tiopronin-MPC carboxylic acid groups and the electron acceptor *N*-(methyl)-*N'*-(ethylamine)-viologen dinitrate ( $\text{MEAV}^{+2}(\text{NO}_3^-)_2$ ) and the fluorophore 5-(aminoacetamido)-fluorescein were demonstrated. The synthetic products of these reactions were investigated with  $^1\text{H}$  and  $^{31}\text{P}$  NMR, capillary electrophoresis, voltammetry, electrochemical quartz crystal microgravimetry, and fluorescence spectroscopy.

(6) For a recent review, see the following: (a) Hostetler, M. J.; Murray, R. W. *Curr. Opin. Coll. Interface Sci.* **1997**, *2*, 42–49. (b) Templeton, A. C.; Wuelfing, W. P.; Murray, R. W., Submitted for publication.

(7) (a) Hostetler, M. J.; Green, S. J.; Stokes, J. J.; Murray, R. W. *J. Am. Chem. Soc.* **1996**, *118*, 4212–4213. (b) Green, S. J.; Stokes, J. J.; Hostetler, M. J.; Pietron, J. J.; Murray, R. W. *J. Phys. Chem. B* **1997**, *101*, 2663–2668. (c) Ingram, R. S.; Hostetler, M. J.; Murray, R. W. *J. Am. Chem. Soc.* **1997**, *119*, 9175–9178. (d) Templeton, A. C.; Hostetler, M. J.; Kraft, C. T.; Murray, R. W. *J. Am. Chem. Soc.* **1998**, *120*, 1906–1911. (e) Templeton, A. C.; Hostetler, M. J.; Warmoth, E. K.; Chen, S.; Hartshorn, C. M.; Krishnamurthy, V. M.; Forbes, M. D. E.; Murray, R. W. *J. Am. Chem. Soc.* **1998**, *120*, 4845–4849. (f) Buining, P. A.; Humbel, B. M.; Philipse, A. P.; Verkeij, A. J. *Langmuir* **1997**, *13*, 3921–3926.

(1) Templeton, A. C.; Chen, S.; Gross, S. M.; Murray, R. W. *Langmuir* **1999**, *15*, 66–76.

(2) Brust, M.; Walker, M.; Bethell, D.; Schiffrin, D. J.; Whyman, R. J. *Chem. Soc., Chem. Commun.* **1994**, 801–802.

(3) Hayat, M. A., Ed. *Colloidal Gold: Principles, Methods, and Applications*; Academic Press: New York, 1989; Vol. 1.

(4) Schon, G.; Simon, U. *Colloid Polym. Sci.* **1995**, *273*, 101–117, 202–218.

(5) Haberland, H., Ed. *Clusters of Atoms and Molecules*; Springer-Verlag: New York, 1994.

**Table 1.** Place-Exchange and Coupling Reactions with Tiopronin-MPCs

reaction type, no.	ligand	feed ratio <sup>a</sup>	product ratio <sup>b</sup>
place-exchange, 1		2:1	3.7:1
place-exchange, 2		2:1	5:1
place-exchange, 3		2:1	3.4:1
place-exchange, 4		2:1	3:1
place-exchange, 5		4:1; 21:1	insoluble; no reaction
reaction type	ligand	reaction stoichiometry <sup>c</sup>	percent conversion
amide formation, 6	<i>N</i> -(methyl)- <i>N'</i> -(ethylamine)-viologen dinitrate, MEAV <sup>2+</sup> (NO <sub>3</sub> <sup>-</sup> ) <sub>2</sub> (see Figure 2 for structure)	1:1; 2:1	28% <sup>d</sup> (24) <sup>e</sup> ; 42% <sup>d</sup> (36) <sup>e</sup>
amide formation, 7	5-(aminoacetamido)-fluorescein (see Figure 6 for structure)	0.5:1	8.2% <sup>f</sup> (3.7) <sup>g</sup>

<sup>a</sup> Mole ratio of cluster-bound tiopronin to ligand in exchange solution. <sup>b</sup> Mole ratio of remaining tiopronin to incorporated exchange ligand on final cluster product. <sup>c</sup> Mole ratio of amine monomer relative to tiopronin acid groups in reaction mixture. <sup>d</sup> Percentage of tiopronin acid groups converted to amides as determined by <sup>1</sup>H NMR. <sup>e</sup> Number of amine monomers coupled to the cluster as determined by <sup>1</sup>H NMR. <sup>f</sup> Percentage of tiopronin acid groups converted to amides as determined by UV-vis spectroscopy. This analysis assumes that the molar absorptivity of the fluorophore attached to the cluster is the same as that of the monomer. <sup>g</sup> Number of amine monomers coupled to the cluster as determined by UV-vis spectroscopy.

copy. The voltammetry of MPCs poly-functionalized with electroactive groups has been described previously,<sup>7,8</sup> but this report is the first employing capillary electrophoresis to probe the structural dispersity of MPCs and using fluorescence spectroscopy to analyze a MPC-bound fluorophore.

## Experimental Section

**Chemicals.** The tiopronin-MPCs (which are not completely monodisperse, but can be represented by the *average* composition of Au<sub>201</sub>-Tiopronin<sub>85</sub>) were prepared as described previously (average core diameter of 1.8 nm).<sup>1</sup> 3-Mercaptopropionic acid (98%), 3-mercaptopropylsulfonic acid sodium salt (tech. grade), hexanethiol (98%), and hexadecanethiol (98%) were obtained from Aldrich, coenzyme A (yeast extract, 92%) and glutathione (98%) from Sigma, and 5-(aminoacetamido)-fluorescein (99%) from Molecular Probes (Eugene, OR). House-distilled water was further purified using a Barnstead NANOpure system ( $\geq 18$  M $\Omega$ ). Buffers were prepared according to standard laboratory procedure. Other chemicals were reagent grade and used as received.

**Spectroscopy.** <sup>1</sup>H NMR spectra (in D<sub>2</sub>O) were obtained with a Bruker AMX 200 MHz spectrometer and were processed with a line broadening of 1 Hz to improve the S/N ratio of MPC solution spectra. <sup>31</sup>P NMR spectra (in D<sub>2</sub>O) were obtained with a Bruker Avance spectrometer with pulse frequency set to 162 MHz. A line-broadening factor of 10 Hz was used to improve the S/N ratio of MPC <sup>31</sup>P NMR data. Fluorescence and UV-vis spectra were acquired using a SPEX Fluorolog-3 spectrofluorimeter with right-angle detection and an ATI UNICAM spectrophotometer, respectively.

**Capillary Electrophoresis.** Capillary electrophoresis was performed using a Hewlett-Packard 3D CE instrument with UV diode array detection. The fused silica capillary used was 50  $\mu$ m i.d. and 64 cm in

total length (56 cm to detection cell) and contained an extended path length detection cell (Z configuration). Before each experiment, the capillary was conditioned by hydrodynamic (950 mbar) flushing with 0.1 N NaOH (5 min), water (5 min), and the experimental buffer (10 min). Sample solutions and run buffer were filtered through a Nylon filter cartridge (0.5  $\mu$ m pore size, Millipore) and placed into 1 mL polypropylene sample vials. Cluster samples were prepared in 20 mM sodium borate buffer (pH 9.3) at  $\sim 10^{-5}$  M concentration. Samples were injected hydrodynamically (50 mbar for 4 s) at the high voltage anode and were detected near the grounded cathode with a diode array detector collecting electropherograms at wavelengths ranging from 190 to 600 nm. Data were collected in all experiments in positive polarity mode at 30 kV applied voltage with the capillary cooled to 20  $^{\circ}$ C.

**Place-Exchange Reactions, No. 1–5.** In a typical place-exchange reaction, 50 mg of tiopronin-MPC and the appropriate amount of incoming water-soluble ligand (see Table 1) were co-dissolved in 25 mL of purified water and stirred for  $\sim 72$  h. The place-exchanged clusters were purified by dialysis with cellulose ester membranes as described before.<sup>1</sup> No effort was made to control the pH of the exchange reaction solution. For place-exchanges performed between nonpolar ligands and tiopronin-MPC monolayers, the reaction conditions differed from that above. For place-exchange between hexanethiol and tiopronin-MPC, 50 mg of tiopronin-MPC was dissolved in water, the appropriate amount of hexanethiol (see Table 1) was dissolved in THF, and then the latter added to the aqueous tiopronin-MPC solution such that a 4:1 THF-water mixture was attained. This mixed solvent system was employed to accommodate the solubility of each reactant; reaction workup was as reported earlier.<sup>7a</sup> The place-exchange reaction of tiopronin monomer with hexanethiolate-MPC<sup>9</sup> (this cluster had an *average* composition of Au<sub>145</sub>hexanethiolate<sub>50</sub>) was performed in THF as described before.<sup>7a</sup>

(8) (a) Ingram, R. S.; Murray, R. W. *Langmuir* **1998**, *14*, 4115–4121. (b) Green, S. J.; Pietron, J. J.; Stokes, J. J.; Hostetler, M. J.; Vu, H.; Wuelfel, W. P.; Murray, R. W. *Langmuir* **1998**, *14*, 5612–5619.

(9) Hostetler, M. J.; Wingate, J. E.; Zhong, C.-Z.; Harris, J. E.; Vachet, R. W.; Clark, M. R.; Londono, J. D.; Green, S. J.; Stokes, J. J.; Wignall, G. D.; Glish, G. L.; Porter, M. D.; Evans, N. D.; Murray, R. W. *Langmuir* **1998**, *14*, 17–30.

Following isolation, each reaction product was analyzed using  $^1\text{H}$  NMR spectroscopy in  $\text{D}_2\text{O}$ . The product spectra are as follows: exchange with 3-mercaptopropylsulfonic acid sodium salt (no. 1):  $\delta$  (ppm) = 1.5 (br, 3 H), 2.1 (br, 0.7 H), 3.0 (br, 0.7 H), 3.6 (br, 0.4 H), 3.7 (br, 2.4 H); exchange with 3-mercaptopropionic acid, (no. 2):  $\delta$  (ppm) = 1.5 (br, 3 H), 2.7 (br, 1 H), 3.6 (br, 0.4 H), 3.8 (br, 1.9 H); exchange with Coenzyme A (no. 3),  $\delta$  (ppm) = 0.7 (d, 2.4 H), 1.5 (br, 3 H), 2.4 (br, 0.9 H), 3.3 (br, 2.2 H), 3.6 (br, 0.6 H), 3.8 (br, 2.8 H), 4.2 (br, 1.2 H), 6.0 (br, 0.4 H), 8.3 (d, 0.9 H); exchange with glutathione (no. 4),  $\delta$  (ppm) = 1.5 (br, 3 H), 2.1 (br, 1 H), 2.5 (br, 0.9 H), 3.5 (d, 0.4 H), 3.8 (br, 4 H).

**Synthesis of *N*-(Methyl)-*N'*-(ethylamine)-viologen dinitrate ( $\text{MEAV}^{+2}(\text{NO}_3^-)_2$ ).** The synthesis of  $\text{MEAV}^{+2}(\text{NO}_3^-)_2$  was based on reports by Buttry<sup>10</sup> and Willner.<sup>11</sup> Methyl iodide (0.9 equiv) was refluxed in acetone for 3 h with viologen and the resulting precipitate collected and washed with copious amounts of acetone to remove unreacted starting materials. NMR revealed pure *N*-(methyl)-viologen iodide (in DMSO):  $\delta$  (ppm) = 4.38 (s, 3 H), 8.0 (d, 2.1 H), 8.6 (d, 2.1 H), 8.85 (d, 2 H), 9.1 (d, 2 H). This product was refluxed in acetonitrile for 72 h with a 4-fold excess of bromoethylamine hydrochloride, and afterward the precipitate was collected and washed copiously with acetonitrile to remove un-reacted starting materials. NMR (in  $\text{D}_2\text{O}$ ) revealed pure *N*-(methyl)-*N'*-(ethylamine)-viologen mono-iodine mono-chloride,  $\text{MEAV}^{+2}(\text{I}^-\text{Cl}^-)$ . Ion exchange of the halide counterions to produce the dinitrate salt was performed according to Buttry.<sup>10c</sup>

**Coupling of Amines to Tiopronin-MPCs, No. 6–7.** Amide-coupling reactions were performed as described by Staros et al.<sup>12</sup> In a typical reaction,  $\sim 100$  mg of tiopronin-MPC cluster was dissolved in 30 mL of 50 mM 2-(*N*-morpholino)ethanesulfonic acid (MES) buffer (pH 6.5) and the solution then made 0.1 M in 1-[3-(dimethylamino)propyl]-3-ethylcarbodiimide hydrochloride (EDC) and 5 mM in *N*-hydroxysulfosuccinimide sodium salt. The appropriate amount of either  $\text{MEAV}^{+2}(\text{NO}_3^-)_2$  or 5-(aminoacetamido)-fluorescein (Table 1, entries no. 6 and 7) was added, and the solution was stirred for 24 h. For the  $\text{MEAV}^{+2}(\text{NO}_3^-)_2$  reaction, the reaction mixture containing the now poly-functionalized cluster was dialyzed as described above. The 5-(aminoacetamido)-fluorescein reaction product was rotovapped to dryness and the cluster collected on a frit and washed with copious amounts of DMF to remove unreacted reagents. NMR spectral assignments for the  $\text{MEAV}^{+2}(\text{NO}_3^-)_2$  reaction product are found in Figure 2; those for the 5-(aminoacetamido)-fluorescein reaction product are (in  $\text{D}_2\text{O}$ ):  $\delta$  (ppm) = 1.5 (br, 3 H), 3.6 (br, 1.8 H), 5.8 (br, 0.1 H), 6.5 (br, 0.15 H), 7.0 (br, 0.03 H), 7.6 (br, 0.03 H), 8.3 (br, 0.015 H).

**Electrochemical Measurements.** (a) Voltammetric measurements were performed using a BAS 100B/W electrochemical analyzer. A single compartment cell contained the working, Pt coil counter and Ag/AgCl reference electrodes, and degassed and  $\text{N}_2$ -blanketed 0.1 M borate buffer (pH 9.2) solutions that were 1 mM in either  $\text{MEAV}^{+2}(\text{NO}_3^-)_2$  monomer or in  $\text{MEAV}^{2+}$  units on  $\text{MEAV}^{+2}(\text{NO}_3^-)_2$ -functionalized MPC. Gold working electrodes (1.6 mm and 10  $\mu\text{m}$  diameter) were polished with 0.5  $\mu\text{m}$  diamond paste (Buehler), followed by rinsing with water, ethanol, and acetone, successively. A cyclic voltammogram in 0.5 M  $\text{H}_2\text{SO}_4$  was used to determine the cleanliness of the electrode surface prior to each experiment.<sup>13</sup> For experiments employing hexadecanethiol-modified gold electrodes, a monolayer was formed on the electrode surface by placing the freshly cleaned electrode in an ethanol solution 1 mM in hexadecanethiol for 24 h and then washing with ethanol and acetone immediately prior to use. (b) Electrochemical quartz crystal microbalance experiments (EQCM) were performed using a Hewlett-Packard 53131A Universal Counter, an HP-E 3616A Power Supply, an oscillator of local design,<sup>14</sup> and an

Ensmann EI400 bipotentiostat, all integrated and controlled using a PC with Labview 4.0. The 5 MHz Au electrode quartz crystal (Maxtek Inc., Torrance, CA) was mounted in a sealed cell using a no. 9 *o*-ring joint. The active area of the Au QCM working electrode was 0.37  $\text{cm}^2$ , including the electrode tab. The mass sensitivity in liquid,  $C_F$ , of 42  $\text{Hz cm}^2/\mu\text{g}$ , determined by silver plating, was in agreement with previous studies.<sup>14,15</sup>

## Results and Discussion

### Place-Exchange Reactions and Product Characterization.

Place-exchange of thiolate ligands is an experimentally simple and versatile synthetic route to *poly-homo*<sup>7a</sup> and *poly-hetero*-functionalized<sup>7c</sup> alkanethiolate MPCs. Thus functionalized alkanethiolate-MPCs have further been shown to participate in  $\text{S}_\text{N}2$ <sup>7d</sup> and coupling<sup>7e</sup> (amide and ester) reactions, leading to the facile incorporation of a broad range of additional chemical tags and probes onto the outer surface of the MPC moiety.

Leaning on the straightforward nature of previous<sup>7a-c</sup> place-exchange reaction chemistry of alkanethiolate-MPCs, similar reactions of water-soluble tiopronin-MPCs are explored in the present report, as reported in Table 1, Entries no. 1–5. Entries no. 1 and 2 are place-exchange reactions of tiopronin-MPCs with thiols that are separated from a polar terminal group by a short methylene spacer. The relative amount of original tiopronin remaining on the MPC and of incorporated exchange ligand on the exchange product (“product ratio”, as assessed by NMR) was typically about one-half of that based on the “reaction feed ratio” (mole ratio of cluster-bound tiopronin to ligand in exchange solution) and assuming a nonselective ligand exchange. For example, in Entry no. 1, a 2:1 mole reaction feed ratio of cluster-bound tiopronin to 3-mercaptopropylsulfonic acid produces MPCs having a mole product ratio of 3.7 tiopronin ligands to 1 sulfonic acid-substituted ligand. Stated differently, each individual MPC product has an average of 18 newly incorporated sulfonic acid-substituted ligands, comprising 22% of the total number of ligands attached to the cluster surface (there are  $\sim 85$  ligands/MPC on the tiopronin-MPCs of the size considered in this study). This extent of observed place-exchange was, for a given reactant feed ratio and reaction time, similar to that seen previously in reactions, in nonpolar organic solvents, of  $\omega$ -functionalized alkanethiols with alkanethiolate-MPCs.<sup>7a-c</sup>

Steric bulkiness of incoming ligands has been shown<sup>7c,16</sup> to affect the extent of place-exchange in reactions of  $\omega$ -alkanethiols with alkanethiolate-MPCs. Steric effects were, however, not evident, or at least not obvious, in aqueous tiopronin-MPC experiments. Thus, the place-exchange reactions of bulky, thiol-containing biomolecules (Entries no. 3 and 4, Table 1) with tiopronin-MPCs yield product ratios similar to those observed for shorter ligands (i.e., Entries no. 1 and 2). The absence of an obvious steric effect is especially interesting for glutathione (Entry no. 4), in which the thiol site is flanked by two short peptide chains. The several possible (and nonexclusive) explanations for the lack of obvious steric effects (relative to previous results in nonpolar solvents) include the following: (a) differing solvation effects in the different solvent media, (b) hydrogen bonding stabilization in tiopronin monolayers,<sup>1</sup> and (c) a greater preponderance of exchange at edge and vertex (“defect”) sites (where steric bulk is of less import) on the tiopronin-MPCs.<sup>16</sup> There could also be effects on the extent and rate of place-exchange of charged ligands due to solution ionic strength and pH; these effects were not examined in the present report.

(10) (a) De Long, H. D.; Buttry, D. A. *Langmuir* **1990**, *6*, 1319–1322. (b) De Long, H. D.; Buttry, D. A. *Langmuir* **1992**, *8*, 2491–2496. (c) Tang, X.; Schneider, T. W.; Walker, J. W.; Buttry, D. A. *Langmuir* **1996**, *12*, 5921–5933.

(11) (a) Katz, E.; Itzhak, N.; Willner, I. *Langmuir* **1993**, *9*, 1392–1396. (b) Doron, A.; Katz, E.; Willner, I. *Langmuir* **1995**, *11*, 1313–1317.

(12) Staros, J. V.; Wright, R. W.; Swingle, D. M. *Anal. Biochem.* **1986**, *156*, 220–222.

(13) Woods, R. In *Electroanalytical Chemistry*; Bard, A. J., Ed; Marcel Dekker: New York, 1980; Vol. 9, p 1.

(14) Cliffel, D. E.; Bard, A. J. *Anal. Chem.* **1998**, *70*, 1993–1998.

(15) Hillier, A. C.; Ward, M. D. *Anal. Chem.* **1992**, *64*, 2539–2554.

(16) Hostetler, M. J.; Templeton, A. C.; Murray, R. W. *Langmuir* **1999**, *15*, 3782–3789.



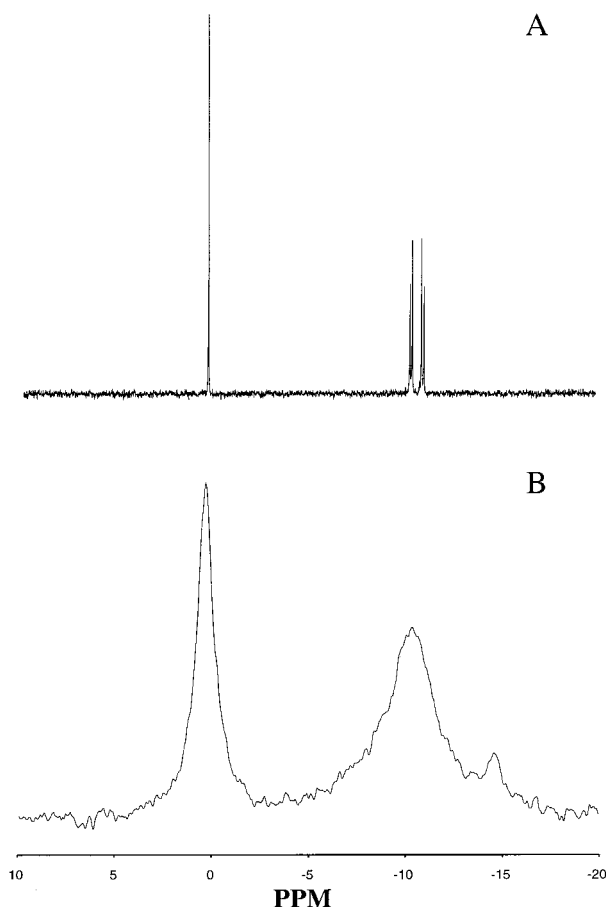


**Figure 1.**  $^{31}\text{P}$  NMR spectra (in  $\text{D}_2\text{O}$ ) of Coenzyme A as (a) the monomer and (b) attached to the cluster. The chemical shifts in both spectra are referenced to phosphoric acid.

Proton and  $^{13}\text{C}$  NMR are powerful tools for assaying ligand structure and proportion in MPC monolayer shells and provide a significant investigative edge over monolayers on two-dimensional (“flat”) surfaces.<sup>9,17b,c</sup> The first application of  $^{31}\text{P}$  NMR to MPCs is shown in Figure 1, which compares spectra of Coenzyme A as a monomer in solution and as attached (by place-exchange) to a tiopronin-MPC (average of 19 Coenzyme A ligands/MPC, Table 1, no. 3). The monomer spectrum (Figure 1a) shows splitting between the two interior phosphate groups ( $\delta = -10$ ) and a singlet for the sugar phosphate group ( $\delta = 0$ ). The cluster  $^{31}\text{P}$  NMR spectrum (Figure 1b) exhibits peaks which are broadened but which lie at the same chemical shifts; the broadening causes the interior phosphate doublet to be unresolved. The peak broadening in the cluster spectrum presumably reflects spin–spin relaxation ( $T_2$ ), as opposed to other noted contributions to broadening in  $^1\text{H}$  and  $^{13}\text{C}$  NMR spectra of alkanethiolate-MPC solutions.<sup>17</sup>

Figure 1b exhibits a peak not observed in the Coenzyme A monomer solution, lying  $\sim 4$  Hz upfield of the interior phosphate peak ( $\delta = -14$ ). This peak comprises 10% of the overall

resonance intensity. Given the well-known acid lability of the interior Coenzyme A phosphate ester groups<sup>18</sup> and considering that mildly acidic conditions were encountered in the place-exchange reaction, it is likely that this new peak arises from some (degraded) Coenzyme A cluster ligands which have been shortened by phosphate ester hydrolysis. Besides detecting such side products, changes in chemical shift or increased broadening in  $^{31}\text{P}$  NMR resonances may prove useful in detecting binding of biomolecules to functionalized receptor sites on MPCs.

Table 1, Entry no. 5 illustrates exchange of a very nonpolar ligand. Place-exchange reactions of tiopronin-MPCs with hexanethiol were performed (for solubility reasons) in 4:1 THF–water. A 4:1 feed ratio (expected tiopronin–hexanethiolate product ratio of  $\sim 8:1$ ) led to a cluster product that was insoluble in water and in a wide range of polar and nonpolar organic solvents. Incorporation of very hydrophobic ligands clearly serves to disrupt the factors contributing to the water solubility of the tiopronin-MPCs. A very lean reaction feed ratio (21:1, aimed at incorporation of only 2–3 hexanethiolate ligands) gave a product exhibiting negligible place-exchange. The opposite reaction, that is, the place-exchange of tiopronin monomer onto hexanethiolate-MPCs at a relatively reaction high feed ratio (2:1), also gave (by  $^1\text{H}$  NMR) no evidence for exchange. These results show that place-exchange of thiolate ligands into protecting monolayers of opposite polarity (for the two cases considered in this study) is highly unfavorable and, when forced to occur, can produce intractably insoluble products.

Place-exchange reactions represent one method to functionalize tiopronin-MPCs and can be used to generate clusters bearing a portfolio of chemically interesting groups (sulfonate, primary amine, tertiary amine). Another attractive functionalization approach is to use the terminal carboxylic acid groups of the tiopronin ligands as amide-forming coupling sites to attach other interesting groups to MPCs.<sup>7e</sup> As noted before,<sup>7e</sup> coupling reactions are also attractive by avoiding synthesis of thiolated versions of the groups of interest; such syntheses can sometimes be troublesome.

**Amide-Forming Coupling Reactions.** Entries no. 6 and 7 (Table 1) are examples of forming amides from the tiopronin-MPC carboxylic acid groups. The reactions utilize the water-soluble carbodiimide, 1-[3-(dimethylamino)-propyl]-3-ethylcarbodiimide hydrochloride (EDC),<sup>19</sup> to catalyze reactions between tiopronin-MPC acid groups and amine-containing electroactive or fluorescent molecules. This catalyst has been used to promote the coupling of the carboxylic acid groups of water-soluble biopolymers such as proteins and oligonucleotides to various fluorescent labels and is widely used to immobilize substrates on affinity chromatography stationary phases.<sup>20</sup> We included *N*-hydroxysulfosuccinimide in the reaction mixture to improve the efficiency of the carbodiimide-mediated amide-forming reaction by producing hydrolysis-resistant active ester reaction intermediates.<sup>21</sup>

**(A) Viologen-MPCs.** The electroactive moiety amide-coupled to tiopronin MPCs was *N*-(methyl)-*N'*-(ethylamine)-viologen dinitrate (abbrev. MEAV<sup>+2</sup>(NO<sub>3</sub><sup>-</sup>)<sub>2</sub>). Viologens of similar structure have been prepared and their electrochemistry examined<sup>21</sup> as Langmuir–Blodgett films<sup>22</sup> and as self-assembled

(17) (a) Peak broadening in  $^1\text{H}$  NMR spectra of alkanethiolate-MPCs has been attributed to core size (spin–spin relaxational broadening ( $T_2$ )), “solid-state” ligand packing density, and chemical shift distributions as a consequence of proximity to the gold core (see following references). The latter two contributions are likely to be small in this case, owing to the distance between the Coenzyme A phosphorous groups and the Au core. (b) Terrill, R. H.; Postlethwaite, T. A.; Chen, C.-H.; Poon, C.-D.; Terzis, A.; Chen, A.; Hutchison, J. E.; Clark, M. R.; Wignall, G.; Londono, J. D.; Superfine, R.; Falvo, M.; Johnson, C. S.; Samulski, E. T.; Murray, R. W. *J. Am. Chem. Soc.* **1995**, *117*, 12537–12548. (c) Badia, A.; Gao, W.; Singh, S.; Demers, L.; Cuccia, L.; Reven, L. *Langmuir* **1996**, *12*, 1262–1269.

(18) March, J. *Advanced Organic Chemistry*; Wiley: New York, 1985.

(19) DeTar, D. F.; Silverstein, R. *J. Am. Chem. Soc.* **1966**, *88*, 1013–1019.

(20) (a) Taniuchi, M.; Clark, H. B.; Johnson, E. M., Jr. *Proc. Natl. Acad. Sci. U.S.A.* **1986**, *83*, 4094–4098. (b) Steers, E. *J. Biol. Chem.* **1971**, *246*, 196.

(21) For reviews of earlier work in the field, see the following: (a) Bird, C. L.; Kuhn, A. T. *Chem. Soc. Rev.* **1981**, *101*, 49–82. (b) Bard, A. J.; Ledwith, A.; Shine, H. J. *Adv. Phys. Org. Chem.* **1976**, *13*, 155.

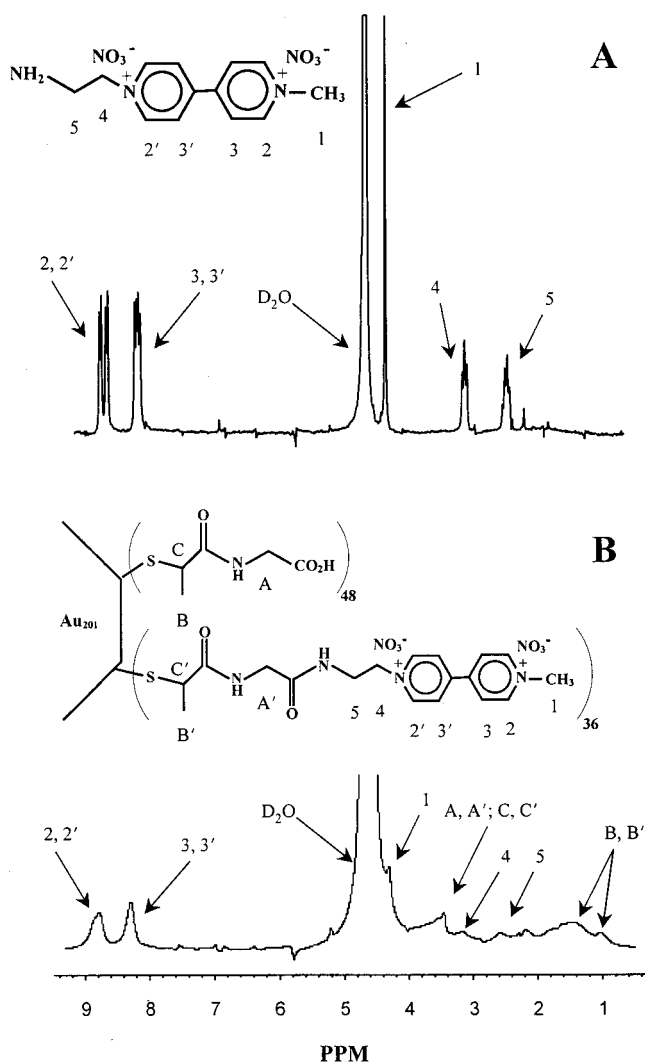


**Figure 2.**  $^1\text{H}$  NMR spectra (in  $\text{D}_2\text{O}$ ) of  $N$ -(methyl)- $N'$ -(ethylamine)-viologen dinitrate,  $\text{MEAV}^{+2}(\text{NO}_3^-)_2$ , as: (a) the monomer and (b) attached to the cluster. For each of the spectra, structures of the molecules are shown and assignments correlating the structure to the spectra are provided.

monolayers on gold.<sup>10,11,23</sup> Entry no. 6, Table 1, shows two amide-coupling experiments, at different reaction feed stoichiometries (mole ratio of amines on  $\text{MEAV}^{+2}(\text{NO}_3^-)_2$  to tiopronin-MPC carboxylic acid groups). Reaction feed ratios 1:1 and 2:1 produced clusters in which 28% and 42% of the carboxylic acid groups had been converted to amides, and which thereby bear on average 24 and 36 viologen sites/MPC, respectively. These relatively heavily labeled clusters are termed below, viologen-MPCs.

Figure 2 shows the  $^1\text{H}$  NMR spectra and peak assignments for the  $\text{MEAV}^{+2}(\text{NO}_3^-)_2$  monomer and of the 36 viologen-MPC poly-functionalized cluster. Peaks in the monomer spectrum (Figure 2a) are sharp and exhibit spin-spin splitting consistent with the structure, whereas those for the cluster (Figure 2b) are

(22) (a) Obeng, Y. S.; Founta, A.; Bard, A. J. *New J. Chem.* **1992**, *16*, 121–129. (b) Oyama, N.; Ikeda, S.; Hatozaki, O.; Shimomura, M.; Mishima, K. *Bull. Chem. Soc. Jpn.* **1993**, *66*, 1091–1097.

(23) (a) Katz, E.; deLacey, A. L.; Fernandez, V. M. *J. Electroanal. Chem.* **1993**, *358*, 261–272. (b) Katz, E.; deLacey, A. L.; Fierro, J. L.; Palacios, J. M.; Fernandez, V. M. *J. Electroanal. Chem.* **1993**, *358*, 247–259. (c) Katz, E.; Itzhak, N.; Willner, I. *J. Electroanal. Chem.* **1992**, *336*, 337. (d) Yau, J.; Li, J.; Chen, W.; Dong, S. *J. Chem. Soc., Faraday Trans.* **1996**, *92*, 1001–1006. (e) Hiley, S.; Buttry, D. A. *Colloids Surf., A* **1994**, *84*, 129–140. (f) Leventis, N.; Sotiriou-Leventis, C.; Chen, M.; Jain, A. J. *Electrochem. Soc.* **1997**, *144*, L305–L308.

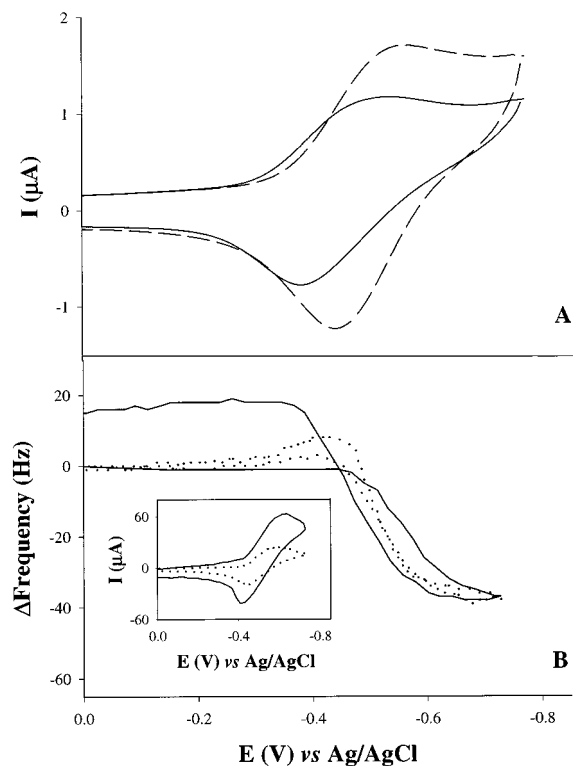


**Figure 3.** (A) Cyclic voltammetry of 1 mM  $\text{MEAV}^{+2}(\text{NO}_3^-)_2$  (---) and 1 mM (in  $\text{MEAV}^{+2}(\text{NO}_3^-)$ ) of cluster poly-functionalized with  $\text{MEAV}^{+2}(\text{NO}_3^-)_2$  (36/cluster, —) in 0.1 M borate buffer (pH 9.2). Both voltammograms are at a scan rate of 50 mV/s at a 1.6 mm diameter Au working electrode. (B) EQCM crystal frequency change vs potential at 10 mV/s (···) and 100 mV/s (—) in 2 mM (in  $\text{MEAV}^{+2}(\text{NO}_3^-)$ ) cluster poly-functionalized with  $\text{MEAV}^{+2}(\text{NO}_3^-)_2$  (36/cluster) in 0.1 M borate buffer (pH 9.2). Corresponding voltammograms for these experiments are shown as insets to the figure.

substantially broadened. Evidence for the success of the coupling reaction is seen by the close correspondence of chemical shifts of peaks (labeled with numbers) for monomer and cluster-bound  $\text{MEAV}^{+2}(\text{NO}_3^-)_2$ ; peaks for protons closest to the new bond (labeled with letters) display a slightly altered chemical shift as would be expected. The absence of sharp peaks in Figure 2b is significant by showing that materials not coupled to the MPCs ( $\text{MEAV}^{+2}(\text{NO}_3^-)_2$  monomer, coupling reagents) have been successfully removed in the purification steps.

**(B) Voltammetry of Viologen-MPCs.** The voltammetry of alkanethiolate-MPCs poly-functionalized with ferrocene, anthraquinone, and phenothiazine has been explored in nonpolar organic solvents,<sup>7,8</sup> but there are as yet no examples of aqueous voltammetry of electroactive MPCs. Figure 3a shows cyclic voltammetry of solutions containing equal concentrations of  $\text{MEAV}^{+2}$  as monomer (---) and as cluster-bound (—), at a macroscopic Au working electrode. The cluster-bound viologens give smaller currents simply because the MPC has a smaller diffusion coefficient than the  $\text{MEAV}^{+2}$  monomer. The  $[\text{viologen}]^{1+/0}$  couple could be observed in aqueous solutions of  $\text{MEAV}^{+2}$  monomer, by suppressing background currents at the Au electrode with a hexadecanethiol monolayer, but this second couple was not observed for cluster-bound  $\text{MEAV}^{+2}$  over the same range of potentials. Further experiments (*vide infra*) indicate adsorption of products in the  $[\text{viologen}]^{2+/1+}$  wave; these may interfere with the second reaction.

Adsorption was detected and quantified using an electrochemical quartz crystal microbalance (EQCM),<sup>24</sup> as shown in Figure 3b. A frequency loss,  $\Delta f$ , of 37 Hz was observed, upon

scanning through the potential interval for the [viologen]<sup>2+/1+</sup> reaction, that was constant at potential scan rates between 10 (•••) and 100 mV/s (—). Assuming that the 37 Hz frequency decrease results from mass deposition on the Au surface, the simplified Sauerbrey<sup>25</sup> equation can be used to find the mass change per area ( $\Delta m/A$ ):

$$\Delta f = -C_f \frac{\Delta m}{A} \quad (1)$$

where  $C_f$  is the sensitivity coefficient (see Experimental Section). Converting the mass change per area ( $\Delta m/A$ ) into  $\Gamma$  (mol/cm<sup>2</sup>) using an average cluster molecular weight of 66 kDa, leads to  $\Gamma = 1.3 \times 10^{-11}$  mol/cm<sup>2</sup>, which corresponds roughly to a single, loosely packed monolayer of cluster on the electrode surface.<sup>26</sup> Methyl viologen has been shown to deposit a single monolayer in previous EQCM studies on its first reduction step;<sup>27</sup> the adsorption behavior of cluster-bound MEAV<sup>+2</sup> is thus unsurprising given its structural similarity. The consistency of the frequency change with changing scan rate (10 to 100 mV/s) argues also that the monolayer formation is rapid.

It is evident in Figure 3b that, as the potential is subsequently scanned positively and oxidation removes the monolayer, the QCM frequency rises but overshoots. (A slight overshoot in frequency was also observed for the negative portion of the 10 mV/s voltammetric scan.) The frequency returns to the initially observed value, given sufficient time at the starting potential. The amount of frequency overshoot was  $\sim 18$  Hz at 100 mV/s potential scan rate and  $\sim 8$  Hz at 10 mV/s. Two possible reasons for the frequency overshoot are the following: (a) the density/viscosity of the solution layer nearest the QCM temporarily increases upon removal of the monolayer because of high localized cluster concentration,<sup>28</sup> and/or (b) a partial MPC monolayer resides on the electrode prior to beginning the experiment. Weak (submonolayer) adsorption of methyl viologen dication has been shown on Au surfaces previously.<sup>29</sup>

Figure 4 shows microelectrode voltammetry of solutions of monomer (---) and cluster-bound MEAV<sup>+2</sup> (—). Three further observations can be made from these data. First, the [viologen]<sup>+2/+1</sup> couple is more positive ( $-0.546$  V) for cluster-bound MEAV<sup>+2</sup> than the MEAV<sup>+2</sup> monomer ( $-0.640$  V). (This difference also appears in the voltammetry of Figure 3a.) There are other, previous examples of positive shifts in [viologen]<sup>+2/+1</sup> couple formal potential (compared to solution viologen species) when the viologens have been forced into some kind of proximity to one another.<sup>22</sup> A positive 86 mV potential has been reported for viologens immobilized on poly(acrylic acid) chemically modified electrodes.<sup>23a</sup> Bard and co-workers observed even larger positive shifts (250 mV) in viologen surfactant Langmuir–Blodgett films.<sup>22a</sup> The origin of this interesting effect has not been established with surety; the most common explanation points to differing degrees of stabilization of the two viologen oxidation states.<sup>21–23</sup> The relative stabilization of reduced viologen in concentrated local environments

(24) Buttry, D. A. In *Electroanalytical Chemistry*; Bard, A. J., Ed; Marcel Dekker: New York 1991; Vol. 17, p 1.

(25) Sauerbrey, G. *Z. Phys.* **1959**, *155*, 206.

(26) Assuming the average cluster composition determined from <sup>1</sup>H NMR in Figure 2b with average molecular weight of 66 kDa and a projected footprint of  $\sim 3$  nm diameter, the calculated amount of cluster in a hexagonally close packed monolayer would be  $2.2 \times 10^{-11}$  mol/cm<sup>2</sup>.

(27) (a) Shimazu, K.; Yanagida, M.; Uosaki, K. *J. Electroanal. Chem.* **1993**, *350*, 321–327. (b) Ostrom, G. S.; Buttry, D. A. *J. Electroanal. Chem.* **1988**, *256*, 411–431.

(28) Lee, W.-W.; White, H. S.; Ward, M. D. *Anal. Chem.* **1993**, *65*, 3232–3237.

(29) Enea, O. *Electrochim. Acta* **1985**, *30*, 13–16.

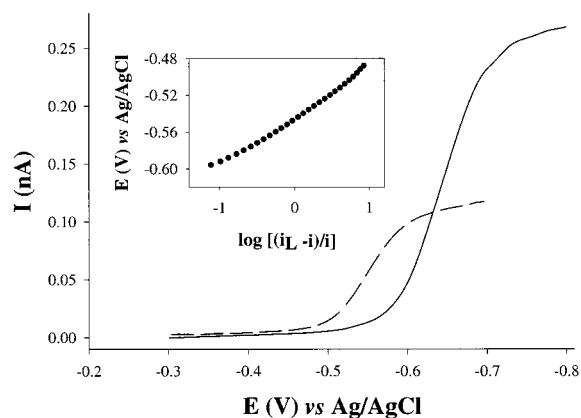


**Figure 4.** Current–potential curves for 1 mM MEAV<sup>+2</sup>(NO<sub>3</sub><sup>−</sup>)<sub>2</sub> (---) and 1.7 mM (in MEAV<sup>+2</sup>(NO<sub>3</sub><sup>−</sup>)<sub>2</sub>) of cluster poly-functionalized with MEAV<sup>+2</sup>(NO<sub>3</sub><sup>−</sup>)<sub>2</sub> (36/cluster, —) in 0.1 M borate buffer (pH 9.2). Both curves were recorded at a scan rate of 1 mV/s at a 10  $\mu$ m Au working electrode. Upper inset: Plot of  $E$  vs  $\log[(i_L - i)/i]$  for the cluster current–potential curve.

implies some form of viologen–viologen interaction or dimerization.<sup>22a</sup> A strong pH dependence of reduction potentials of thin viologen films has also been reported,<sup>23b</sup> whereas no pH dependence of the [viologen]<sup>+2/+1</sup> step occurs in the voltammetry of soluble viologen derivatives.<sup>21a</sup> Voltammetry of cluster-bound MEAV<sup>+2</sup> in aqueous solutions of ionic strength similar to that in Figure 4 is, however, independent of pH at values ranging from 5 to 10.

Second, the limiting current  $I_{LIM}$  of the microelectrode voltammetry in Figure 4 yields the cluster diffusion coefficient,  $D$ , and hydrodynamic radius,  $r_H$ , using the following equations:<sup>30</sup>

$$I_{LIM} = 4nFrDC\theta_{SITES} \quad \text{and} \quad r_H = \frac{kT}{6\pi\eta D} \quad (2)$$

where  $n = 1$  for the [viologen]<sup>+2/+1</sup> reaction,  $F$  is the Faraday constant,  $C$  is the MPC concentration,  $\theta_{SITES}$  is the average number of viologens per MPC (we assume based on other work that all react<sup>30</sup>),  $k$  is the Boltzmann constant,  $T$  is temperature, and  $\eta$  is solution viscosity. The  $I_{LIM}$  values give  $D = 3.1 \times 10^{-6}$  cm<sup>2</sup>/s for the cluster and  $1.1 \times 10^{-5}$  cm<sup>2</sup>/s for the monomer. The latter result is consistent with previous studies of viologen derivatives.<sup>21</sup> The cluster diffusion coefficient leads to a hydrodynamic radius,  $r_H$ , of 0.7 nm, which is clearly unreasonably small given that the average core radius is about 0.9 nm. Measures of  $r_H$  for alkanethiolate-MPCs using the same approach have also produced values lower than expected. The effect suggests some additional contributions to the measured voltammetric currents;<sup>7,8</sup> at least one factor could be the electrons required for intrinsic gold core double layer charging as the core potential is made to traverse the potentials bounding the viologen wave.<sup>31</sup>

Third, the voltammetric waveshape in Figure 4 can be analyzed on the basis of a reversible electrode reaction of the

(30) Wightman, R. M.; Wipf, D. O. In *Electroanalytical Chemistry*; Bard, A. J., Ed; Marcel Dekker: New York, 1989; Vol. 15, p 271.

(31) (a) Ingram, R. S.; Hostetler, M. J.; Murray, R. W.; Schaaf, T. G.; Khoury, J.; Whetten, R. L.; Bigioni, T. P.; Guthrie, D. K.; First, P. N. *J. Am. Chem. Soc.* **1997**, *119*, 9279–9280. (b) Chen, S.; Ingram, R. S.; Hostetler, M. J.; Pietron, J. J.; Murray, R. W.; Schaaf, T. G.; Khoury, J. T.; Alvarez, M. M.; Whetten, R. L. *Science* **1998**, *280*, 2098–2101. (c) Chen, S.; Murray, R. W.; Feldberg, S. W. *J. Phys. Chem. B* **1998**, *102*, 9898–9907.



cluster-bound MEAV<sup>+2</sup> using the following equation:<sup>32</sup>

$$E = E_{1/2} + \frac{0.059}{n} \log \left[ \frac{i_{\text{lim}} - i}{i} \right] \quad (3)$$

The inset shows the appropriate plot with its linear central portion ( $r^2 = 0.99$ ) and slope of 53 mV. A similar analysis of the MEAV<sup>+2</sup> monomer voltammetry (data not shown) is also linear with a slope of 61 mV. A small dispersity of the cluster-bound viologens' formal potentials could lead to the slight curvature in the plot (analogous to that seen for ferrocenated alkanethiolate clusters<sup>7b,8b</sup>). Another factor contributing to both curvature and slope difference from the ideal 59 mV value is uncertainty caused by the sloping post-reduction portion of the experimental data. The currents continue to slope upward at more negative potentials and probably reflect slow hydrogen reduction processes.

Finally, the oxidative scan in microelectrode cyclic voltammetry at very slow potential scan rates (1 mV/s, data not shown) exhibits a large stripping wave with a charge of magnitude indicating that cluster multilayers have formed. Adsorption of viologen-MPC was also investigated by EQCM on longer time scales using potential step experiments in which the potential was stepped past the first viologen reduction (0 to  $-0.83$  V vs Ag/AgCl) and held for 120 s, while concomitantly monitoring the QCM frequency change (data not shown). A rapid frequency decrease similar ( $\sim 37$  Hz) to that seen in Figure 3b confirmed the rapidity of cluster monolayer formation. This initial rapid change was followed by a slow continual decrease in QCM frequency of  $\sim 15$  Hz; this additional mass implies formation of multiple layer(s) of adsorbed cluster and, thus, the existence of significant *inter-cluster* viologen–viologen interactions (*vide supra*).

**(C) Dispersity in Viologen-MPCs; Capillary Electrophoresis.** It is important to appreciate that not all of the tiopronin-MPC or viologen-MPC cluster molecules are identical. It is common that large, poly-functional molecules have some level of dispersity (e.g., functionalized polymers). We know<sup>1</sup> (TEM) that tiopronin-MPCs exhibit dispersity in the size of the Au core; the Au<sub>201</sub> composition is an average value. There may be dispersity in the number of tiopronin ligands even on a given core size; whether this occurs is not known. There is almost certainly dispersity in the number of amide bonds formed to different clusters in reactions such as that (Table 1, Entry no. 6) producing the viologen-MPCs. Ways to detect and investigate these monolayer dispersities are badly needed. The water solubility of the MPCs in the present study provided an opportunity to apply the considerable resolving power of capillary electrophoresis to the dispersity problem.

Capillary electropherograms of solutions of tiopronin-MPC and tiopronin-MPC poly-functionalized with 36 MEAV<sup>+2</sup>(NO<sub>3</sub><sup>-</sup>)<sub>2</sub> groups (Table 1, no. 6) are shown in Figure 5, panels a and b, respectively. These experiments were performed in 20 mM sodium borate buffer at pH 9.3 and were run in the presence of a neutral marker (mesityl oxide, labeled with an asterisk). At pH 9.3, all of the tiopronin acid groups should be deprotonated, while the charges of the cluster-bound MEAV<sup>+2</sup> groups do not vary with pH.

Figure 5 clearly illustrates the dispersity of the two kinds of MPC samples. The electropherogram of the tiopronin-MPC sample is a partially resolved envelope of overlapping peaks. As noted above, the tiopronin-MPC Au core diameter (1.8 ±

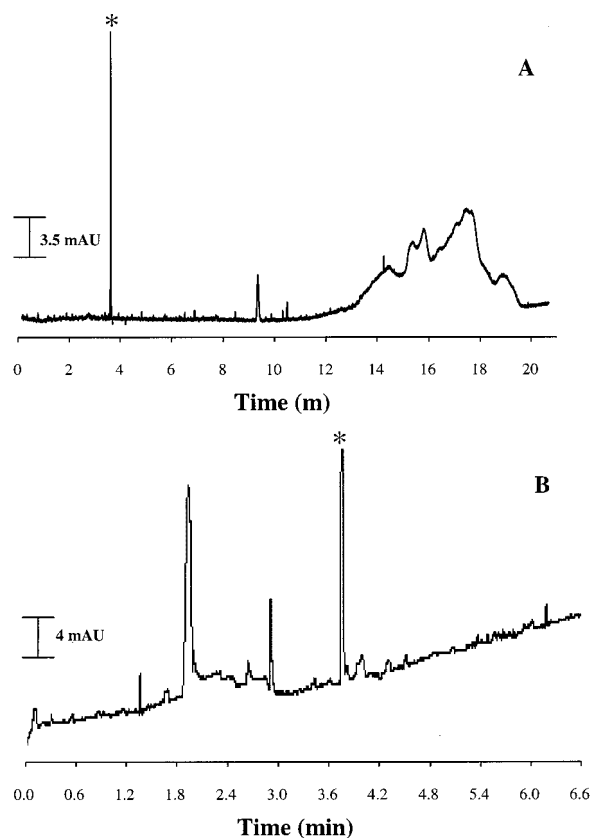


**Figure 5.** (a) An electropherogram of a  $3.3 \times 10^{-5}$  M solution of tiopronin-MPC. (b) An electropherogram of a  $6.8 \times 10^{-5}$  M solution of tiopronin cluster with 36 attached MEAV<sup>+2</sup>(NO<sub>3</sub><sup>-</sup>)<sub>2</sub> groups. Both samples are in 20 mM sodium borate buffer (pH 9.3) and were detected at 192 nm with a UV diode array detector. A 9-point Savitsky-Golay smoothing routine was applied to both of the raw electropherograms. The peak labeled with an asterisk (\*) is the neutral marker (mesityl oxide).

0.7 nm)<sup>1</sup> and possibly the number of ligands/MPC are expected to exhibit dispersity. The multiple peaks in the electropherogram must reflect an assortment of separable core size/ligand number/charge state combinations. Although these combinations are unknown, average properties can be taken from the Figure 5 data. The average electrophoretic mobility,  $\mu_{\text{EP}}$ , of the cluster sample<sup>33</sup> can be calculated from

$$\mu_{\text{EFF}} = \mu_{\text{EO}} + \mu_{\text{EP}} \quad (4)$$

where  $\mu_{\text{EFF}}$  is the effective electrophoretic mobility of the sample and  $\mu_{\text{EO}}$  is a measure of electroosmotic flow taken from the position of the neutral marker. The tiopronin-MPC peaks in Figure 5a yield electrophoretic mobility ( $\mu_{\text{EP}}$ ) values ranging from  $-3.8$  to  $-4.3 \times 10^{-4}$  cm<sup>2</sup> V<sup>-1</sup> s<sup>-1</sup> (avg.  $-4.2 \times 10^{-4}$  cm<sup>2</sup> V<sup>-1</sup> s<sup>-1</sup>). The electrophoretic mobility of the tiopronin-MPC relative to the neutral marker ( $\mu_{\text{EO}} = 5.3 \times 10^{-4}$  cm<sup>2</sup> V<sup>-1</sup> s<sup>-1</sup>) shows that the net charge on the tiopronin-MPC is negative. The electrophoretic mobility can be related to the average cluster charge,  $Z$ , by<sup>33</sup>

$$\mu_{\text{EP}} = \frac{Ze}{6\pi\eta r_{\text{H}}} \quad (5)$$

where  $e$  is the electronic charge ( $1.61 \times 10^{-19}$  C),  $\eta$  is the solution viscosity (0.01 g cm<sup>-1</sup> s<sup>-1</sup>), and  $r_{\text{H}}$  is again the average

(32) Bard, A. J.; Faulkner, L. R. *Electrochemical Methods: Fundamentals and Applications*; John Wiley & Sons: New York, 1980.

(33) (a) Jorgenson, J. W.; Lukacs, K. D. *Anal. Chem.* **1981**, 53, 1298–1302. (b) Jorgenson, J. W.; Lukacs, K. D. *Science* **1983**, 222, 266–272.

cluster hydrodynamic radius, which from a combination of core radius and ligand size we assume to be  $\sim 1.5$  nm. Equation 5 yields an average, effective cluster charge of  $Z = -7.4$ , far less than the average total of 85 ionized carboxylic acids-MPC. It is expected, however, that the multiple charges of each tiopronin-MPC will be substantially screened by the surrounding ionic space charge formed by the buffer electrolyte; this is a well-known effect in low ionic strength solutions of polyacid macromolecules.<sup>34</sup> We have seen an analogous effect in the electrolyte concentration sensitivity of  $pK_A$ 's observed in titrations of tiopronin-MPCs.<sup>1</sup>

Figure 5b provides an electropherogram for a tiopronin-MPC poly-functionalized with 36 MEAV<sup>+2</sup>(NO<sub>3</sub><sup>-</sup>)<sub>2</sub> groups, making the total charge of the average composition to be +23 overall (e.g., Au<sub>201</sub>Tiopronin<sup>-</sup><sub>49</sub>MEAV<sup>+2</sup><sub>36</sub>). The average electrophoretic mobility ( $\mu_{EP}$ ) of this material is, from eq 4,  $+4.6 \times 10^{-4}$  cm<sup>2</sup> V<sup>-1</sup> s<sup>-1</sup> relative to the neutral marker. Note the change in the sign of the net charge, which is expected from the MPC composition. This value of electrophoretic mobility yields a hydrodynamic radius of 1.5 nm and an average effective cluster charge of  $Z = +8.1$ . Use of the diffusion coefficient obtained from microelectrode voltammetry ( $D = 3.1 \times 10^{-6}$  cm<sup>2</sup> s<sup>-1</sup>) in the alternative equation<sup>33</sup>

$$\mu_{EP} = \frac{ZeD}{kT} \quad (6)$$

produces  $Z = +3.7$ , which is within a factor of 2 of the calculation involving an assumed hydrodynamic radius value. Again, the effective charge is substantially less than the expected actual one, owing to screening by the ionic space charge formed around the charged cluster.

The electropherogram of the cluster poly-functionalized with MEAV<sup>+2</sup> (Figure 5b) differs from that of tiopronin-MPCs (Figure 5a) in being composed of a dominant, rather sharp peak riding atop a shallow, broadened peak. Migration time differences ( $t_m$ ) alone are insufficient to account for the narrowness of this peak (relative to that in Figure 5a). The spatial variance of a peak,  $\sigma_1$ , is given by the Einstein equation<sup>32</sup>

$$\sigma_1 = \sqrt{2Dt_m} \quad (7)$$

and major differences in  $D$  between tiopronin-MPCs and viologen-MPCs are unexpected. The difference in the peak width in Figure 5, panels a and b, can thus be taken as reflecting a real difference in the dispersity of the two materials.

It is attractive to imagine using electrophoretic mobilities to probe the poly-dispersity of core sizes in a given cluster preparation, but this is complicated by the connection between the number of charges (e.g., ligands) and the core size. For example, assuming a constant MPC charge over the cluster peak in Figure 5a ( $Z = -7.4$ ) produces estimates of hydrodynamic values ranging from 1.45 to 1.65 nm. These values do not, however, adequately represent the wider extent of core size variance that is measured by TEM ( $1.8 \pm 0.7$  nm). Hence, combined uncertainties in charge and hydrodynamic radius assumptions prohibit exact determinations of either from the capillary electrophoresis experiments. These experiments are nonetheless promising in that they provide the first wedge into high-resolution separation of poly-disperse water-soluble MPCs. Addressing the full potential of the separation experiment will

(34) Johnson, C. S., Jr.; He, Q. In *Advanced Magnetic Resonance*; Warren, W. W., Ed.; Academic Press: New York, 1989; Vol. 13, pp 131–159.

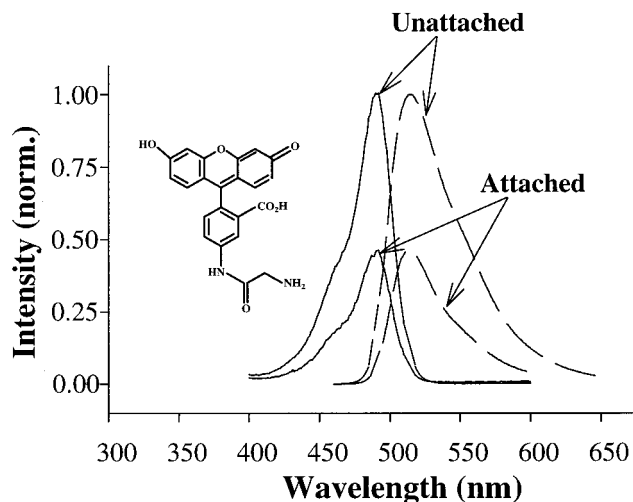


**Figure 6.** Excitation ( $\lambda = 515$ , —) and emission ( $\lambda = 490$ , - - -) spectra of  $0.5 \mu\text{M}$  5-(aminoacetamido)-fluorescein monomer (upper set of labeled curves) and  $0.5 \mu\text{M}$  (in fluorophore) of cluster poly-functionalized with 5-(aminoacetamido)-fluorescein (lower set of labeled curves,  $0.013 \mu\text{M}$  in cluster). Both spectra were acquired in 50 mM phosphate buffer (pH 7.5). The chemical structure of 5-(aminoacetamido)-fluorescein is shown to the left in the figure for reference.

require independent measurements of charge and core size, such as capillary electrophoresis interfaced to mass spectrometry.

**(D) Fluorescein-MPCs.** Fluorescence spectroscopy is a cornerstone of modern analytical biochemistry because of its high sensitivity and the development of facile labeling strategies for attaching fluorophores to biomolecules.<sup>35</sup> Fluorescein and its derivatives are prominent in such studies because of their high absorptivity, excellent quantum yield, and good water solubility.<sup>36</sup> Entry no. 7 of Table 1 provides results for the carbodiimide catalyzed coupling of 5-(aminoacetamido)-fluorescein to the carboxylic acid groups of tiopronin-MPCs. The number of fluorophores coupled to the clusters (3.7 fluorophores-MPC, termed below, fluorescein-MPC) was measured using UV-vis spectrophotometry, since it was judged to be a more accurate measure than <sup>1</sup>H NMR for determining a small number of coupled sites. The attachment of fluorophores to MPCs has been achieved previously,<sup>7e,f</sup> but this study describes the first fluorescence spectroscopy of MPC-bound fluorophores.

Excitation (solid line) and emission (dashed line) spectra are shown in Figure 6 for fluorescein monomer and the fluorescein-MPC cluster. The upper curves (see labels) in Figure 6 correspond to the excitation ( $\lambda = 515$  nm, —) and emission ( $\lambda = 490$  nm, - - -) spectra of a  $0.5 \mu\text{M}$  solution of the 5-(aminoacetamido)-fluorescein monomer (structure shown in Figure 6). The bottom curves (see labels) in Figure 6 correspond to the excitation ( $\lambda = 515$  nm, —) and emission ( $\lambda = 490$  nm, - - -) spectra of  $0.5 \mu\text{M}$  (in fluorophore) of cluster-bound 5-(aminoacetamido)-fluorescein (fluorescein-MPC). The excitation spectra of the monomer and cluster-bound fluorescein are identical in shape and wavelength maxima. Likewise, the emission spectra of the monomer and cluster-bound fluorescein also bear strong resemblance. Importantly, the fluorescence spectrum of a solution of monomer is unchanged (data not shown) by the addition of (unlabeled) tiopronin-MPC at the same cluster

(35) Lacowicz, J. R., Ed. *Principles of Fluorescence Spectroscopy*; Plenum: New York, 1983.

(36) Haugland, R. P. *Handbook of Fluorescent Probes and Research Chemicals*; Molecular Probes: Eugene, Oregon, 1996.



concentration as in Figure 6, indicating no quenching or self-absorption effects at these concentrations.

The only difference between the fluorescence spectrum of fluorescein monomer and fluorescein-MPC is that the latter's intensity is about 50% smaller. Given the absence of any quenching in a fluorescein + tiopronin-MPC solution, the intensity difference must reflect effects associated with the attachment of the fluorescein to the MPC. The basis of such an effect needs further study, but one obvious possibility is energy transfer quenching by the metal-like gold core. This is under further investigation.

Understanding the reactivity of water-soluble gold clusters is a prerequisite to exploring their applications as biosensors, as components of rationally designed nanoscale electronic

devices, and as electron-transfer mediators for biological reactions. This paper has established two facile routes to poly-functionalized water-soluble gold clusters. The generality of the place-exchange and amide-coupling poly-functionalization reactions sets the stage for the further exploration of nanoscale cluster molecules in an aqueous environment.

**Acknowledgment.** This work was supported in part by grants from the National Science Foundation (NSF) and Office of Naval Research (ONR). The authors thank Kate Hutterer and Prof. Gary Pielak (U.N.C.) for helpful discussions. A.C.T. acknowledges support from Dobbins and Lord Corporation Fellowships.

JA990513+